Risk of Scar in the Comparison of Age-related Macular Degeneration Treatments Trials

Ebenezer Daniel, MBBS, PhD,[1] Cynthia A. Toth, MD,[2] Juan E. Grunwald, MD,[1] Glenn J. Jaffe, MD,[2] Daniel F. Martin, MD,[3] Stuart L. Fine, MD,[4] Jiayan Huang, MS,[1] Gui-shuang Ying, MD, PhD,[1] Stephanie A. Hagstrom, PhD,[3] Katrina Winter, BS,[2] Maureen G. Maguire, PhD,[1] for the Comparison of Age-related Macular Degeneration Treatments Trials Research Group*

Objective: To describe risk factors for scar in eyes treated with ranibizumab or bevacizumab for neovascular age-related macular degeneration (AMD).

Design: Prospective cohort study within a randomized clinical trial.

Participants: Patients with no scar on color fundus photography (CFP) or fluorescein angiography (FA) at enrollment in the Comparison of Age-related Macular Degeneration Treatments Trials (CATT).

Methods: Eyes were assigned to ranibizumab or bevacizumab treatment and to 1 of 3 dosing regimens for 2 years. Masked readers assessed CFP and FA. Baseline demographic characteristics, visual acuity, morphologic features on photography and optical coherence tomography (OCT), and genotypes associated with AMD risk were evaluated as risk factors using adjusted hazard ratios (aHRs) and associated 95% confidence intervals (CIs). Scars were classified as fibrotic with well-demarcated elevated mounds of yellowish white tissue or nonfibrotic with discrete flat areas of hyperpigmentation with varying amounts of central depigmentation.

Main Outcome Measures: Scar formation.

Results: Scar developed in 480 of 1059 eyes (45.3%) by 2 years. Baseline characteristics associated with greater risk of scarring were predominantly classic choroidal neovascularization (CNV) (aHR, 3.1; CI, 2.4–3.9) versus occult CNV, blocked fluorescence (aHR, 1.4; CI, 1.1–1.8), foveal retinal thickness >212 μm (aHR, 2.4; CI, 1.7–3.6) versus <120 μm, foveal subretinal tissue complex thickness >275 μm (aHR, 2.4; CI, 1.7–3.6) versus ≤75 μm, foveal subretinal fluid (aHR, 1.5; CI, 1.1–2.0) versus no subretinal fluid, and subretinal hyperreflective material (SHRM) (aHR, 1.7; CI, 1.3–2.3) versus no SHRM. Eyes with elevation of the retinal pigment epithelium had lower risk (aHR, 0.6; CI, 0.5–0.8) versus no elevation. Drug, dosing regimen, and genotype had no statistically significant association with scarring. Fibrotic scars developed in 24.7% of eyes, and nonfibrotic scars developed in 20.6% of eyes. Baseline risk factors for the scar types were similar except that eyes with larger lesion size or visual acuity <20/40 were more likely to develop fibrotic scars.

Conclusions: Approximately half of eyes enrolled in CATT developed scar by 2 years. Eyes with classic neovascularization, a thicker retina, and more fluid or material under the foveal center of the retina are more likely to develop scar. *Ophthalmology 2014;121:656-666 © 2014 by the American Academy of Ophthalmology.*

Subretinal and retinal scarring are associated with profound vision loss and are natural outcomes of neovascular age-related macular degeneration (nvAMD).[1–4] Because untreated choroidal neovascularization (CNV) progresses from a neovascular bundle to a variably mixed fibrovascular structure and eventually culminates in a scar, it causes local destruction of photoreceptors, retinal pigment epithelium (RPE), and choroidal blood vessels, leading to permanent alteration in macular morphology and reduction in vision. Eyes that develop fibrosis after photodynamic therapy for CNV have poor vision outcomes.[5] Scar that develops after radiotherapy for nvAMD has been described.[6,7] However, treatment patterns for nvAMD have changed in the past decade, and nearly all patients now receive treatment with intravitreal injections of drugs that target vascular endothelial growth factor (VEGF).[8] Although anti-VEGF treatment generally stabilizes or improves visual acuity, scar formation has been identified as one of the causes of visual acuity loss after treatment.[9]

The factors associated with scarring after anti-VEGF therapy have not been described. In the Comparison of Age-related Macular Degeneration Treatments Trials (CATT), a multicenter clinical trial sponsored by the National Eye Institute, approximately 1200 patients were treated with the anti-VEGF drugs ranibizumab and bevacizumab and followed closely with visual acuity testing, optical coherence tomography (OCT), color fundus photography (CFP), and fluorescein angiography (FA). We describe the morphologic features of scars that evolve after anti-VEGF treatment, their incidence through 2 years of treatment, and associated baseline risk factors.

Methods

Enrollment and Follow-up of Subjects

Between February 2008 and December 2009, 1185 patients were enrolled in CATT through 43 clinical centers in the United States. Each patient had untreated active CNV secondary to age-related macular degeneration (AMD) in 1 eye, designated as the study eye. Inclusion and exclusion eligibility criteria and baseline morphologic features have been described previously.[10] Key inclusion criteria included age ≥50 years and visual acuity between 20/25 and 20/320 in the study eye. At study entry, active CNV was considered present when both leakage on FA and fluid on time-domain OCT were documented through central image review.[11,12] The neovascular complex or fluid needed to be under the fovea. At enrollment, scar at the foveal center was an exclusion criterion, but eyes with nonfoveal scarring that was <50% of the total CNV lesion were eligible. Patients were randomly assigned to treatment with intravitreal injections of ranibizumab or bevacizumab to 1 of 3 dosing regimens for the 2 years of the study: monthly injections, monthly evaluation with injection only when signs of active neovascularization were present (pro re nata [PRN]), or monthly evaluation for 1 year followed by PRN injections for 1 year. Patients were examined approximately every 28 days.[10] Stereoscopic CFP, FA, and OCT scans were obtained at baseline, 1 year, and 2 years. Eyes receiving PRN therapy had monthly OCT scans. An institutional review board associated with each center approved the clinical trial protocol. All patients provided written informed consent. The study was compliant with Health Insurance Portability and Accountability Act regulations. The CATT was registered with ClinicalTrials.gov (NCT00593450).

Assessment of Images

Methods used to grade digital CFP, FA, and OCT scans in CATT have been described previously.[11,12] At baseline, images were assessed for the following features: type of CNV; presence of contiguous hemorrhage, serous pigment epithelial detachment, or blocked fluorescence that was not due to hemorrhage; pathology at the foveal center; presence of CNV or scar in the fellow eye; and presence of geographic atrophy in both the study eye and the fellow eye. The area of CNV and the total CNV lesion was measured using Image J (available at http://rsbweb.nih.gov/ij/; Rasband WS, ImageJ, US National Institutes of Health, Bethesda, MD, 1997−2012). Identification of scar was based only on CFP and FA characteristics. Two broad scar categories were identified: fibrotic scars and nonfibrotic scars.

Fibrotic scars were defined as obvious white or yellow mounds of fibrous-appearing tissue that were well defined in shape and appeared solid on color stereo images. Figure 1A shows CNV at baseline with a dome-shaped subretinal hyperreflective material (SHRM) developing into a yellowish-brown solid fibrotic scar with a smaller and irregular SHRM at year 2. Hyperfluorescence due to tissue staining or blocked fluorescence of the underlying choroid was present on FA. When fibrotic scars were admixed with active neovascularization, there was leakage on angiography (Fig 1A).[13] Other imaging modalities (e.g., OCT) may reveal characteristics that are not discernible on CFP and FA. Figure 1B illustrates classic CNV that does not involve the foveal center on FA, but SHRM on the OCT extends under the fovea. At 2 years, the CFP shows the developing fibrotic scar extending into the foveal center and beyond the baseline CNV area (Fig 1B5). The scar is hypofluorescent early and stains minimally in the late-phase FA (Fig 1B6, B7). The OCT scan at year 2 shows flattening of SHRM (Fig 1B8) overlying retinal thinning, loss of the photoreceptor outer segments, ellipsoid zone, and external limiting membrane. This case illustrates that in some cases the extent of classic CNV at baseline is better visualized by OCT than FA and may be an important feature in predicting whether a developing fibrotic scar is likely to involve the foveal center. Furthermore, the loss of outer retinal layers highlights the anatomic reasons for poor visual acuity typically associated with scar formation.

Nonfibrotic scars were typically flat, small, well-circumscribed areas of pigmentation with varying degrees of central hypo-pigmentation on CFP images (Fig 2). The peripheral pigmentary changes in these scars often followed the outline of the previously active CNV lesion. The hypopigmented area was flat, and choroidal vessels were not visible. Hyperfluorescence of the depigmented area appeared early on FA and persisted or increased in intensity in the late phase. Hypofluorescence on FA surrounding the hyperfluorescence corresponded to the pigmented borders apparent on CFP. In rare instances, flat yellowish areas with or without clearly demarcated hyperpigmented borders in the area of baseline CNV were present and classified as nonfibrotic scars (Fig 2C1−C8).

The location of fluid (intraretinal, subretinal, and sub-RPE); thickness at the foveal center of the retina, subretinal fluid, and subretinal tissue complex; presence of SHRM; RPE elevation; epiretinal membrane; and vitreomacular attachment were determined from OCT B-scan cross-sections. Time-domain OCT was performed at baseline through 1 year, and time-domain OCT or spectral-domain OCT was performed during the second year. The SHRM, RPE, and RPE elevation, excluding subretinal fluid, comprised the subretinal tissue complex.

Candidate Risk Factors

Candidate risk factors for scarring included baseline demographic characteristics, history of cigarette smoking, hypertension, diabetes, dietary supplementary use, cancers, hypercholesterolemia, osteoarthritis, anti-VEGF drug and regimen, visual acuity in the study eye and fellow eye, and glaucoma, as well as the morphologic features graded by the reading centers. Five single nucleotide polymorphisms (SNPs) previously associated with risk and progression of AMD were evaluated as risk factors for incident scar: (1) complement factor H Y402H (rs1061170), (2) age-related maculopathy susceptibility 2 (also called *LOC387715*) A69S (rs10490924), (3) high temperature requirement factor A1 (rs11200638), (4) complement component 3 R80G (rs2230199), and (5) toll-like receptor 3 (rs3775291).

Statistical Methods

Only subjects without scar at baseline were included. Each candidate risk factor, except for the SNPs, was first evaluated by univariate analysis (without adjustment for any other risk factors) using a discrete time Cox proportional hazard model for time to scar. The predictors with a $P < 0.20$ in the univariate analysis were included in a multivariate Cox proportional hazard model so that the independent effect of each predictor could be assessed. Treatment regimen was included as a time-dependent covariate to accommodate the treatment regimen re-randomization at 1 year for the patients treated monthly. The final multivariate model was created by applying a backward selection procedure that retained only those predictors with a $P < 0.05$, with the exception of drug and regimen groups, which were included in all multivariate models. Adjusted hazard ratios (aHRs) for scar development during 2 years and their 95% confidence intervals (CIs) were calculated on the basis of the final multivariate models. Similar analyses were performed separately for fibrotic scars and nonfibrotic scars. The association of scar formation and the number of risk alleles for
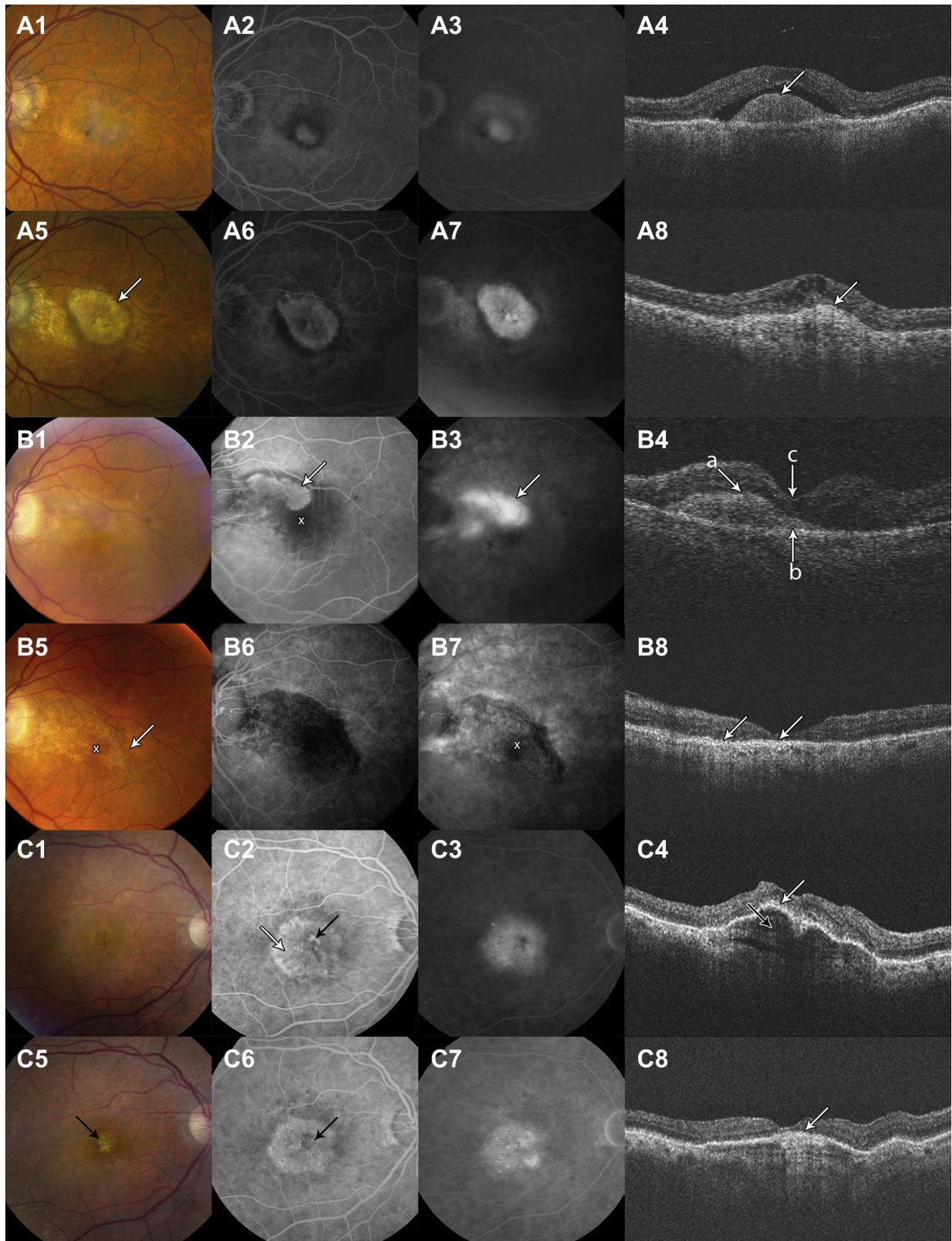
Figure 1.

each specific SNP was assessed with a logistic regression model that included age, sex, and smoking status. *P* values for the genetic analysis were adjusted to control for the false discovery rate.[14] All data analyses were performed using SAS version 9.3 (SAS Inc., Cary, NC).

Results

After excluding patients with scar at baseline (n = 46) and those without gradable photographs at both 1 and 2 years because of death, missed visits, or poor photograph quality (n = 80), there were 1059 patients eligible for scar risk factor analysis (Fig 3, available at www.aaojournal.org). At the end of 1 year, 339 eyes (32.0%) had developed a scar, and after 2 years of anti-VEGF therapy, 480 eyes (45.3%) had developed a scar.

The results of the univariate analysis are shown in Tables 1 to 3 (available at www.aaojournal.org). By univariate analysis, the risk factors associated with increased risk of scar were poor baseline visual acuity in the study eye; larger baseline CNV area; minimally and predominantly classic CNV; blocked fluorescence on angiography; hemorrhage associated with the lesion (included hemorrhage within and contiguous with the lesion, measured as approximate disc areas); greater retinal thickness, subretinal tissue complex thickness at the foveal center; and presence of intraretinal and subretinal fluid and SHRM. Factors associated with lower risk of scar were worse visual acuity in the fellow eye, retinal angiomatous proliferation (RAP) and geographic atrophy in the study eye, sub-RPE fluid, and RPE elevation. Systemic diseases, such as diabetes, hypertension, and hypercholesterolemia, were not associated with scar formation.

In the multivariate final model, several baseline features independently predicted scarring (Table 4). Eyes with predominantly classic CNV on FA (aHR, 3.1; 95% CI, 2.4−3.9) and minimally classic CNV on FA (aHR, 2.3; 95% CI, 1.8−3.0) had higher risk when compared with eyes with only occult CNV. This is illustrated in Figure 1C, where a small area of baseline classic CNV within a large occult CNV lesion (C2, white arrow) develops into a small yellow fibrotic scar at year 2. No scar development can be seen on CFP or FA in the area of the baseline occult CNV. The CNV lesions with blocked fluorescence had a higher risk when compared with CNV lesions without blocked fluorescence (aHR, 1.4; 95% CI, 1.1−1.8). Eyes with retinal thickness at the foveal center >212 μm on OCT (aHR, 2.4; 95% CI, 1.7−3.6) or retinal thickness between 120 and 212 μm (aHR, 1.6; 95% CI, 1.1−2.3) had higher risk than eyes with retinal thickness <120 μm. Risk of scarring increased with greater subretinal tissue complex thickness (*P* < 0.0001). Eyes with subretinal fluid in the foveal center had higher risk compared with eyes with no subretinal fluid in the foveal center (aHR, 1.5; 95% CI, 1.1−2.0). Risk was greater for eyes with SHRM (aHR, 1.7; 95% CI, 1.3−2.3) and less for eyes with RPE elevation (aHR, 0.6; 95% CI, 0.5−0.8). The frequency of scar development was similar for the 2 anti-VEGF drugs, bevacizumab compared with ranibizumab (aHR, 1.2; 95% CI, 0.96−1.4), and for the dosing regimens, PRN compared with monthly (aHR, 0.9; 95% CI, 0.8−1.1).

Fibrotic Scars and Nonfibrotic Scars

At the end of 2 years of anti-VEGF therapy, 262 patients (24.7%) developed fibrotic scar; 205 (19.4%) developed fibrotic scar by 1 year, and an additional 57 (5.4%) developed fibrotic scar by the end of 2 years. The cumulative incidence rates of fibrotic scar at 1 and 2 years were 0.19 (95% CI, 0.17−0.22) and 0.26 (95% CI, 0.24−0.29), respectively. At the end of 2 years, 218 subjects (20.6%) developed nonfibrotic scar; 134 (12.7%) developed nonfibrotic scar by 1 year, and an additional 84 (7.9%) developed nonfibrotic scar by the end of 2 years. The cumulative incidence rates of nonfibrotic scar at 1 and 2 years were 0.13 (95% CI, 0.11−0.15) and 0.24 (95% CI, 0.21−0.27), respectively.

Several OCT characteristics at year 2 were associated with fibrotic and nonfibrotic scarring at the foveal center. The OCT characteristics among eyes with fibrotic scar at the foveal center, nonfibrotic scar at the foveal center, and no scar or an extrafoveal scar are quantified in Table 5. Eyes with geographic atrophy at the foveal center were excluded from this analysis because their thickness measurements could be abnormally low. Mean thickness of the retina and subretinal fluid at the foveal center was similar among the 3 groups. The mean thickness of the subretinal tissue complex at the foveal center was greatest (168 μm; standard error [SE], 8.7) for eyes with fibrotic scars, less (148 μm; SE, 14.5) for eyes with nonfibrotic scars, and least (119 μm; SE, 4.1) for eyes with no scar at the foveal center (*P* < 0.0001). Intraretinal fluid at the foveal center was more common in eyes with fibrotic scar (65%) than in eyes with nonfibrotic scars or no scar (46.3% and 48.1%, respectively; *P* < 0.0001). Subretinal fluid was less common in eyes with fibrotic scar (24%) than in eyes with nonfibrotic or no scar (46.3% and 38.8%, respectively; *P* < 0.004). Sub-RPE fluid was less common in eyes with fibrotic scar (20.7%) and nonfibrotic scar (25.9%) than in eyes with no scar at the foveal center (41.9%; *P* < 0.001). Mean visual acuity score in letters at the end of 2 years was 57.6 (∼20/80) among 150 eyes with a fibrotic scar at the foveal center, 67.5 (∼20/50) among 54 eyes with a nonfibrotic scar at the foveal center, and 71.8 (∼20/40) among 680 eyes with no scar in the foveal center (*P* < 0.001).

Presence of a scar in the fellow eye at baseline did not substantially increase the risk of scarring in the study eye. At 2 years, among 133 patients with a scar in the fellow eye at baseline, 36 (27%) had a fibrotic scar, 17 (13%) had a nonfibrotic scar, and 80 (60%) had no scar in the study eye. In contrast, among 926 patients who did not have a fibrotic scar in the fellow eye at baseline, fibrotic scar developed in 226 (24%), nonfibrotic scar developed in 201 (22%), and no scar developed in 499 (54%; *P* = 0.06).

Risk factors for fibrotic and nonfibrotic scar development relative to those without any scarring are presented in Table 6. All of the factors identified for the combined group of fibrotic and nonfibrotic scars were identified as risk factors for fibrotic scars alone, plus 2 additional features were identified. Worse initial visual acuity and larger lesion size were associated with increased risk of fibrotic scars compared with eyes without any scarring. Some of the factors identified for the combined group of scars were not significantly

---

Figure 1. Development of fibrotic scar from classic choroidal neovascularization (CNV). **A,** Choroidal neovascularization at baseline developing into a fibrotic scar at 2 years. **B,** Classic CNV seen on color fundus photography and fluorescein angiography (FA) at baseline does not extend into the foveal center (*white X*), whereas baseline optical coherence tomography shows subretinal hyperreflective material under the fovea (**B4,** *white arrows*). Color fundus photographs and FA at 2 years show a fibrotic scar extending into the foveal center and beyond the baseline CNV. **C,** Baseline early FA (**C2**) shows leakage (*black arrow*) that characterizes classic CNV within a large occult CNV lesion (**C2,** *white arrow*). Optical coherence tomography shows retinal pigment epithelium (RPE) elevation with a hyperreflective "onion peel" appearance in the sub-RPE space that corresponds to the occult lesion (**C4,** *black arrow*). At 2 years, there is a small yellow fibrotic scar (**C5** , *black arrow*) at the site of the baseline classic CNV. There is no fibrous scarring in the area of occult CNV. Optical coherence tomography shows flattening of the RPE elevation (**C8,** *white arrow*) and a persisting "onion-peel" appearance in the subretinal space.
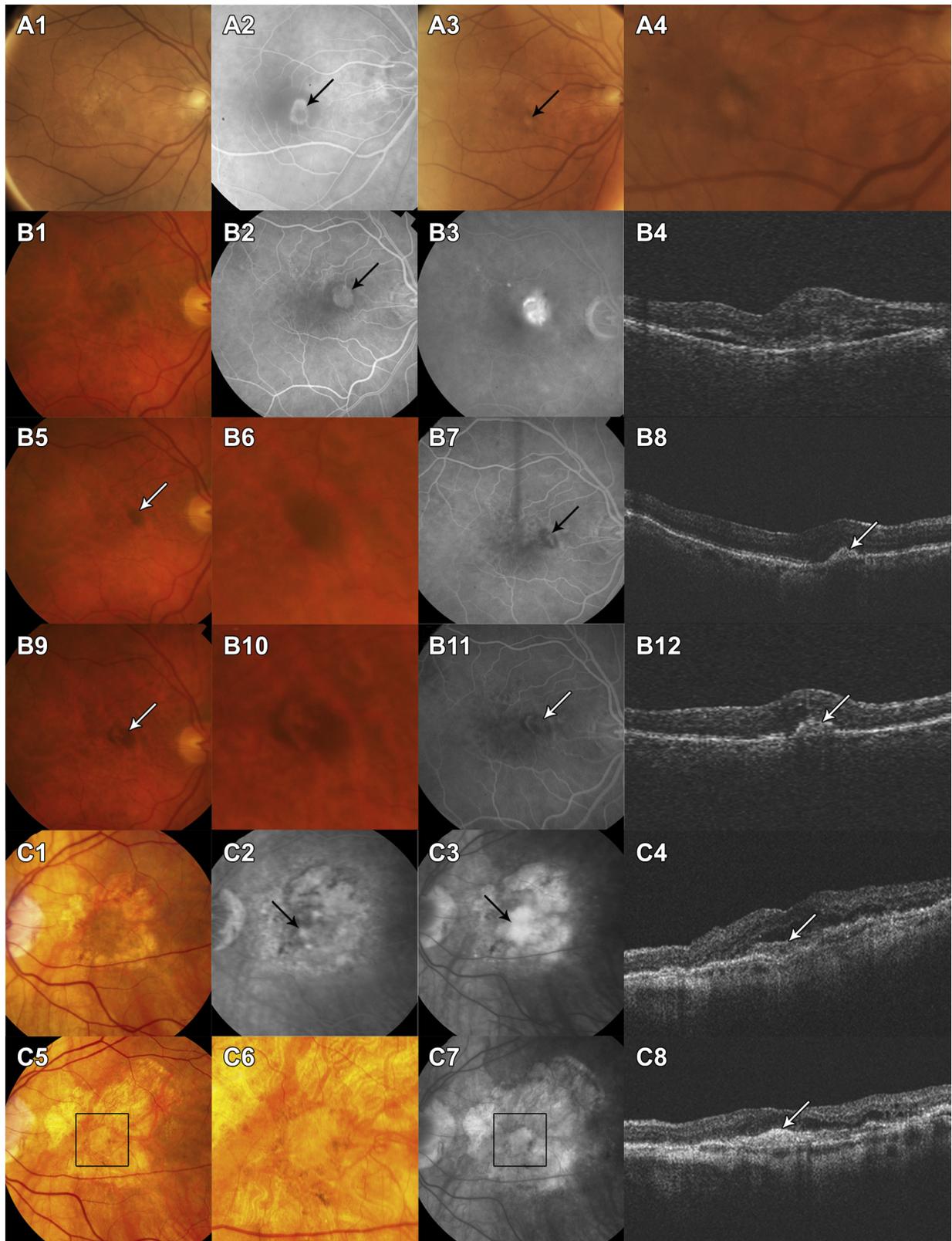
Figure 2.

associated with the risk of nonfibrotic scars alone (Table 6, italics). However, the hazard ratios were in the same direction (i.e., >1.00 or <1.00) as the hazard ratios for fibrotic scars. Although a larger area of CNV was associated with increased risk of fibrotic scar, it was associated with decreased risk of nonfibrotic scar. Eyes with classic CNV and eyes with SHRM were at higher risk of both types of scar. There was minimal association between a scar of either type and drug or treatment regimen.

There was no significant relationship between scar development and the 5 SNPs that were evaluated. A stepwise analysis also failed to show a significant interaction among the number of risk alleles present. Adjusting for age, sex, and smoking habits did not alter these results (Table 7).

Discussion

After 1 year, scar developed in one third of the eyes treated with anti-VEGF drugs, and by 2 years, approximately half the eyes developed scar. We identified baseline characteristics that predicted scar formation: classic CNV, blocked fluorescence on FA, increased retinal thickness, foveal subretinal fluid, and SHRM. The type of anti-VEGF therapy and dosing regimen did not strongly influence scar development. Moreover, commonly described AMD genotypes were not associated with increased risk of scarring.

In our study, it was important to characterize the nature of the scar observed on CFP and FA because these specific features had predictive value of visual acuity and did not always conform to definitions specified in earlier studies.[7,15,16] Fibrotic scars were relatively easy to recognize as raised mounds of white or yellowish tissue that were well defined in shape and appeared solid on color stereo images.[13] Nonfibrotic scars were typically flat, depigmented lesions with varying amounts of signet-shaped peripheral dark pigmentation that conformed to the baseline CNV area. On OCT, nonfibrotic scars, as defined by CFP and FA, often had hyperreflective material in a subretinal or sub-RPE location that would be consistent with fibrosis. Also, the foveal center thickness of the subretinal tissue complex in eyes with a nonfibrotic scar was between the thickness of eyes with fibrotic scars and those with no scar, that is, those having foveal CNV, fluid, or no pathology.

We avoided using terms such as "disciform scar" and "atrophic scar," which were used in some reports.[13–15] Disciform scar implies a disc-shaped, circular fibrotic scar,[17–19] an appearance that was rarely seen on CATT photographic images after 1 or 2 years of anti-VEGF therapy. In a previous study, "atrophic scar" was used to describe flat or slightly concave areas of uniformly depigmented RPE with well-defined borders through which large choroidal vessels are visible.[16] These atrophic scars stained but did not exhibit fluorescein leakage, and their FA characteristics did not correspond to geographic atrophy. In atrophic scars, hyperfluorescence did not begin early as it does in RPE window defects (because there may be a "thin" layer of RPE or fibrous tissue present) and did not fade in the late phase of the angiogram. This presentation is different from nonfibrotic scars that appear as discrete areas of dark hyperpigmentation at the site of the baseline CNV, with varying amounts of central depigmentation with no visible choroidal vessels and the appearance of early hyperfluorescence on FA.

To our knowledge, this report is the first from a large-scale, prospective study to describe in detail the incidence and risk of scars that develop from CNV lesions after PRN or monthly ranibizumab and bevacizumab intravitreal injections. Previous histopathologic and clinical studies of eyes with disciform scars secondary to AMD have documented loss of the majority of the overlying photoreceptors and outer nuclear layer and poor visual function.[2,20–22]

Descriptions of scars in reports from other studies of anti-VEGF treatments have not been detailed or have a short follow-up period and a relatively small number of eyes.[23–27] Reports from MARINA (Minimally Classic/Occult Trial of the Anti-VEGF Antibody Ranibizumab in the Treatment of Neovascular Age-Related Macular Degeneration) and ANCHOR (ANti-VEGF Antibody for the Treatment of Predominantly Classic CHORoidal Neovascularization in AMD Trial) noted that visual acuity loss was not statistically associated with leakage, hemorrhage, or fibrosis in ranibizumab-treated eyes.[16] Our study found that visual acuity was lowest in eyes that developed fibrotic scar involving the foveal center.

An important question that has prognostic and therapeutic implications is whether intravitreal anti-VEGF therapy alters the formation of retinal scar in eyes with nvAMD. The ability of VEGF to regulate scar tissue formation has not been studied extensively. In a study that used fetal and adult wound-healing murine models, scar-free fetal wounds had lower VEGF levels and were less vascular than fibrotic fetal wounds, and the scar-free phenotype was converted to a scar-forming phenotype when exogenous VEGF was added.[28] When VEGF was neutralized in adult wounds, vascularity was reduced, and scar formation was decreased. Bevacizumab is reported to have antifibrotic activity that reduces scar formation in glaucoma filtration surgery.[29–31] Furthermore, as noted earlier, large disciform scars were

Figure 2. Development of nonfibrotic scars. **A,** Classic choroidal neovascularization (CNV) **(A2)** at baseline. At 2 years, color fundus photography (CFP) **(A3, A4)** shows a circumscribed small area of hypopigmentation surrounded by a ring of dark pigmentation. **B,** Classic CNV at baseline **(B1–4)**. Dark pigmentation in the area of the baseline CNV **(B5** and **B6,** *white arrow*) at 1 year. Optical coherence tomography shows retinal pigment epithelium (RPE) elevation with hyperreflective material in the sub-RPE space. At 2 years, an area of hypopigmentation is seen within the darkly pigmented area. **C,** Baseline CFP shows several areas of geographic atrophy around the foveal center. Fluorescein angiogram shows classic CNV (complement component 3) and optical coherence tomography shows subretinal fluid overlying an area of subretinal hyperreflective material **(C4,** *white arrow*). There is increased signal penetration into the choroid. At 2 years, the CFP shows a small, yellow, flat scar in the area of baseline CNV, closely resembling the geographic atrophy (within the *black square* on **C5**). However, unlike the adjacent areas of geographic atrophy, in this region, the choroidal vessels are not visible. Optical coherence tomography shows thickened hyperreflective material **(C8)**. The first 2 examples (A1-A4 and B1-B12) demonstrate the typical appearance of a nonfibrotic scar with signet-shaped hyperpigmentation surrounding an area of hypopigmentation. The last example (C1-C8) shows a flat scar without pigmentation that seems to be an uncommon presentation of nonfibrotic scar.

Table 4. Multivariate Analysis for Incidence of Scar within 2 Years

Baseline Characteristics	Subjects Included in the Final Model (N=1010)	Subjects with Scar at Week 52 or 104, n (%)	Adjusted Hazard Ratio (95% CI)	P Value*
Lesion type				
Occult only	614	183 (29.8)	1.00	<0.0001
Minimally classic	144	90 (62.5)	2.30 (1.76–3.00)	
Predominantly classic	252	188 (74.6)	3.05 (2.40–3.86)	
Blocked fluorescence				
No	872	364 (41.7)	1.00	0.02
Yes	138	97 (70.3)	1.38 (1.07–1.78)	
Retinal thickness at foveal center (μm)				
<120	104	35 (33.7)	1.00	<0.0001
120–212	542	228 (42.1)	1.61 (1.12–2.33)	
>212	364	198 (54.4)	2.44 (1.67–3.56)	
Subretinal tissue complex thickness at foveal center (μm)				
>0–≤75	246	77 (31.3)	1.00	<0.0001
>75–≤160	244	122 (50.0)	1.68 (1.24–2.27)	
>160–≤275	257	134 (52.1)	1.89 (1.39–2.57)	
>275	263	128 (48.7)	2.45 (1.78–3.37)	
Subretinal fluid				
No fluid	175	70 (40.0)	1.00	0.014
Fluid not at foveal center	476	230 (48.3)	1.08 (0.82–1.44)	
Fluid in foveal center	359	161 (44.9)	1.45 (1.08–1.96)	
RPE elevation				
No	133	90 (67.7)	1.00	0.0005
Yes	877	371 (42.3)	0.63 (0.49–0.82)	
SHRM				
No	235	58 (24.7)	1.00	0.0005
Yes	775	403 (52.0)	1.71 (1.26–2.30)	
Drug				
Ranibizumab	525	227 (43.2)	1.00	0.14
Bevacizumab	485	234 (48.3)	1.15 (0.96–1.39)	
Regimen[†]				
Monthly for 2 yrs	252	111 (44.1)	1.00	0.44
Monthly yr 1, PRN yr 2	252	122 (48.4)	—	
PRN for 2 yrs	506	228 (45.1)	0.93 (0.76–1.13)	

CI = confidence interval; PRN = pro re nata; RPE = retinal pigment epithelium; SHRM = subretinal hyperreflective material.
*P values are from a time-dependent Cox proportional hazard model.
[†]Regimen was a time-dependent variable with the value of monthly or PRN.

rarely seen after 2 years anti-VEGF therapy in CATT. The rarity of large fibrotic scars in CATT suggests that extensive fibrosis is aborted or delayed by anti-VEGF therapy. Paradoxically, in eyes with proliferative diabetic retinopathy treated with anti-VEGF injections, there is increased fibrosis caused by imbalances between connective tissue growth factor and VEGF.[32,33] These data suggest that VEGF plays a diverse role in the wound repair process.

Table 5. Association of Optical Coherence Tomography Characteristics at 2 Years with Foveal Center Scar at 2 Years (N=884*)

Optical Coherence Tomography Characteristics	Scarring at the Foveal Center at 2 Years			P Value
	Fibrotic Scar (n=150)	*Nonfibrotic Scar (n=54)*	*No Scar (n=680)*	
Thickness at foveal center, μm, mean (SE)				
Retina	165 (5.88)	152 (9.85)	163 (2.92)	0.58
Subretinal fluid	4.51 (2.27)	11.7 (3.80)	10.7 (1.32)	0.13
Subretinal tissue complex	168 (8.70)	148 (14.5)	119 (4.08)	<0.0001
Fluid at foveal center, n (%)				
Any	118 (78.7)	43 (79.6)	508 (74.7)	0.27
Intraretinal	98 (65.3)	25 (46.3)	327 (48.1)	<0.0001
Subretinal	36 (24.0)	25 (46.3)	264 (38.8)	0.004
Sub-RPE	31 (20.7)	14 (25.9)	285 (41.9)	<0.0001
Visual acuity at yr 2, mean (SE)	57.6 (1.34)	67.5 (2.23)	71.8 (0.63)	<0.0001

RPE = retinal pigment epithelium; SE = standard error.
*Eyes with foveal center geographic atrophy (n = 63) at week 104 were excluded.

Table 6. Multivariate Analysis for Incidence of Fibrotic Scar and Nonfibrotic Scar within 2 Years

Baseline Characteristics	Fibrotic Scar vs. No Scar				Nonfibrotic Scar vs. No Scar			
	Subjects (N=799)	Fibrotic Scar, n (%)	Adjusted Hazard Ratio (95% CI)*	P Value*	Subjects (N=765)	Nonfibrotic Scar, n (%)	Adjusted Hazard Ratio (95% CI)*	P Value*
Baseline visual acuity in study eye								
20/25−40	290	45 (15.5)	1.00	0.004	333	87 (26.1)	1.00	0.33
20/50−80	307	103 (33.6)	1.61 (1.10−2.35)		280	76 (27.1)	0.91 (0.66−1.25)	
20/100−160	152	76 (50.0)	2.14 (1.42−3.22)		121	43 (35.5)	1.12 (0.77−1.62)	
20/200−320	50	26 (52.0)	1.52 (0.86−2.68)		31	7 (22.6)	0.55 (0.25−1.22)	
Baseline area of CNV (disc areas)								
≤1	296	88 (29.7)	1.00	0.019	331	121 (36.6)	1.00	0.04
>1−≤2	173	57 (33.0)	1.70 (1.16−2.50)		152	36 (23.7)	0.77 (0.52−1.15)	
>2−≤4	174	50 (28.7)	1.42 (0.95−2.14)		152	28 (18.4)	0.60 (0.39−0.93)	
>4	88	23 (26.1)	1.24 (0.73−2.12)		77	11 (14.3)	0.48 (0.25−0.91)	
Missing	68	32 (47.1)	2.03 (1.25−3.31)		53	17 (32.1)	1.12 (0.66−1.88)	
Lesion type								
Occult only	516	85 (16.5)	1.00	<0.0001	532	98 (18.4)	1.00	<0.0001
Minimally classic	109	55 (50.5)	2.76 (1.92−3.97)		89	35 (39.3)	2.39 (1.61−3.56)	
Predominantly classic	174	110 (63.2)	4.14 (2.84−6.03)		144	80 (55.6)	3.11 (2.23−4.32)	
Blocked fluorescence								
No	694	186 (26.8)	1.00	0.0004	690	*179 (25.9)*	*1.00*	*0.41*
Yes	105	64 (61.0)	1.84 (1.32−2.58)		75	*34 (45.3)*	*1.18 (0.79−1.75)*	
Retinal thickness at foveal center (μm)								
<120	87	18 (20.7)	1.00	<0.0001	86	*17 (19.8)*	*1.00*	*0.08*
120−212	421	112 (26.3)	1.67 (0.99−2.80)		433	*117 (27.0)*	*1.58 (0.95−2.65)*	
>212	286	120 (42.0)	2.73 (1.60−4.66)		245	*79 (32.2)*	*1.83 (1.07−3.11)*	
Subretinal tissue complex thickness at foveal center (μm)								
>0−≤75	202	33 (16.3)	1.00	<0.0001	214	*45 (21.0)*	*1.00*	*0.11*
>75−≤160	180	58 (32.2)	1.57 (1.00−2.48)		189	*65 (34.4)*	*1.58 (1.07−2.34)*	
>160−≤275	194	71 (36.6)	2.08 (1.32−3.26)		186	*63 (33.9)*	*1.44 (0.96−2.14)*	
>275	223	88 (39.5)	3.11 (1.96−4.94)		175	*40 (22.9)*	*1.18 (0.76−1.83)*	
Subretinal fluid								
No fluid	139	34 (24.5)	1.00	0.012	141	*36 (25.5)*	*1.00*	*0.74*
Fluid not at foveal center	371	125 (33.7)	1.03 (0.68−1.54)		352	*106 (30.1)*	*1.16 (0.79−1.71)*	
Fluid at foveal center	289	91 (31.5)	1.60 (1.04−2.46)		271	*71 (26.2)*	*1.12 (0.75−1.68)*	
RPE elevation								
No	97	54 (55.7)	1.00	<0.0001	79	*36 (45.6)*	*1.00*	*0.07*
Yes	702	196 (27.9)	0.50 (0.36−0.70)		682	*175 (25.7)*	*0.71 (0.49−1.03)*	
SHRM								
No	204	27 (13.2)	1.00	0.008	208	31 (14.9)	1.00	0.004
Yes	595	223 (37.5)	1.82 (1.17−2.83)		557	182 (32.7)	1.78 (1.20−2.64)	
Drug								
Ranibizumab	428	130 (30.4)	1.00	0.85	396	*98 (24.8)*	*1.00*	*0.16*
Bevacizumab	371	120 (32.4)	1.03 (0.78−1.34)		369	*115 (31.2)*	*1.22 (0.93−1.60)*	
Regimen[†]								
Monthly for 2 yrs	205	64 (31.2)	1.00	0.13	189	*48 (25.4)*	*1.00*	*0.81*
Monthly for 1 yr, PRN for 2 yrs	197	67 (34.0)	−		186	*55 (29.6)*	*−*	
PRN for 2 yrs	397	119 (30.0)	0.81 (0.62−1.07)		390	*110 (28.2)*	*1.04 (0.78−1.39)*	

CI = confidence interval; CNV = choroidal neovascularization; PRN = pro re nata; RPE = retinal pigment epithelium; SHRM = subretinal hyper-reflective material.

Note: All results not in italics are from the final multivariate model. The results in italics are from the multivariate model with adjustment of all variables in the final model.

*From a time-dependent Cox proportional hazards model.

[†]Regimen was a time-dependent variable with a value of monthly or PRN.

The type of CNV, as determined by FA at baseline, predicted scar formation. Scars were least likely to develop in eyes with occult CNV only. When occult CNV is admixed with the classic type, the risk doubles. The risk triples when the angiographic phenotype subset is composed predominantly of classic CNV. It is possible that intravitreal anti-VEGF treatment decreases scar formation in purely occult lesions by confining the CNV to the sub-RPE space, thereby stopping progression to classic CNV. Stevens et al[34] reported evidence suggesting that classic CNV increases the risk of development of fibrosis in AMD. The greater propensity for classic CNV to transform into a scar is illustrated in Figure 1C, where the minimally classic lesion's small, centrally located classic CNV changes into

Table 7. Association of Genotype with the Incidence of Scar within 2 Years (N = 797)

SNP[§]	Genotype	Subjects at Risk, n	Scar at Week 52 or 104, n (%)*	Univariate Analysis Hazard Ratio (95% CI)[†]	Adjusted Analysis Hazard Ratio (95% CI)[‡]
CFH rs1061170	CC	258	125 (48.5)	1.01 (0.76–1.34)	1.02 (0.77–1.36)
	TC	370	164 (44.3)	0.90 (0.69–1.18)	0.91 (0.70–1.19)
	TT	169	82 (48.5)	1.00	1.00
	Linear trend P		0.88	0.83	0.77
	Adjusted P[‖]				0.78
ARMS2 rs10490924	TT	163	76 (46.6)	1.06 (0.80–1.42)	1.06 (0.79–1.38)
	GT	371	177 (47.7)	1.11 (0.88–1.40)	1.09 (0.86–1.38)
	GG	263	118 (44.9)	1.00	1.00
	Linear trend P		0.65	0.60	0.64
	Adjusted P[‖]				0.78
HTRA1 rs11200638	AA	155	74 (47.7)	1.10 (0.83–1.48)	1.10 (0.82–1.47)
	AG	371	176 (47.4)	1.10 (0.87–1.39)	1.10 (0.87–1.39)
	GG	271	121 (44.7)	1.00	1.00
	Linear trend P		0.49	0.45	0.48
	Adjusted P[‖]				0.78
C3 rs2230199	GG	55	27 (49.1)	1.06 (0.71–1.59)	1.08 (0.72–1.62)
	CG	303	131 (43.2)	0.84 (0.67–1.04)	0.85 (0.68–1.07)
	CC	439	213 (48.5)	1.00	1.00
	Linear trend P		0.41	0.40	0.52
	Adjusted P[‖]				0.78
TLR3 rs3775291	CC	397	172 (43.3)	0.81 (0.57–1.16)	1.00 (0.70–1.44)
	TC	326	162 (49.7)	0.99 (0.69–1.41)	0.82 (0.57–1.18)
	TT	74	37 (50.0)	1.00	1.00
	Linear trend P		0.10	0.08	0.08
	Adjusted P[‖]				0.48
No. of risk alleles	0–2	85	47 (55.3)	1.00	1.00
	3	112	46 (41.1)	0.67 (0.45–1.01)	0.67 (0.44–1.01)
	4	154	70 (45.5)	0.76 (0.53–1.11)	0.76 (0.52–1.10)
	5	173	81 (46.8)	0.81 (0.56–1.16)	0.82 (0.57–1.17)
	6	136	65 (47.8)	0.86 (0.59–1.25)	0.85 (0.58–1.25)
	≥7	137	62 (45.3)	0.76 (0.52–1.11)	0.76 (0.52–1.12)
	Linear trend P		0.71	0.75	0.78
	Adjusted P[‖]				0.78

ARMS2 = age-related maculopathy susceptibility 2; C3 = complement 3; CI = confidence interval; CFH = complement factor H; HTRA1 = HtrA serine peptidase 1; TLR3 = toll-like receptor 3 gene.
*Linear trend P value is from a logistic regression model with genotype coded as 0, 1, and 2 risk alleles.
[†]Linear trend P value is from proportional hazards model with genotype coded as 0, 1, and 2 risk alleles.
[‡]Linear trend P value is from proportional hazard models adjusted for age, gender, and smoking status.
[§]The risk alleles are C for CFH, T for ARMS2, A for HTRA1, G for C3, and C for TLR3.
[‖]The multiple testing adjusted P values were calculated using the approach of false discovery rate.

a fibrotic scar in the CFP at 2 years, whereas the larger occult portion of the CNV lesion, although active, does not transform to a CFP-visible scar.

The CATT included eyes treated only with anti-VEGF monotherapy. However, in a recent phase II study, eyes were treated with ranibizumab, with or without anti–platelet-derived growth factor therapy (Dugal PU, Reichel E, Boyer DS, et al. Phase 2b trial results show effectiveness of combination therapy. Retina Times. Fall 2012). The results showed that combination therapy more effectively than monotherapy improved visual acuity and better eliminated SHRM. In the present study, we found that SHRM was associated with scar formation. Accordingly, in the future, it will be of interest to determine whether combination therapy similarly reduced the rate of fibrotic or nonfibrotic scar as one explanation for the better visual acuity observed in that study.

Several studies have suggested that CNV sequelae, such as subretinal hemorrhage, are associated with fibrovascular scarring.[35] For example, in one retrospective study, progressive visual acuity loss occurred in 41 eyes of 40 patients with subfoveal subretinal hemorrhage that comprised more than 50% of the CNV lesion.[36] In that report, it was not clear whether the scar formation was directly a result of the more extensive hemorrhage. In contrast, in another study of eyes with nvAMD treated with anti-VEGF therapy, subfoveal fibrosis developed in the absence of significant subfoveal hemorrhage.[37] Likewise, hemorrhage was not associated with the development of scar in CATT. However, blocked fluorescence, defined as blockage of fluorescence that was not associated with pigment or hemorrhage, was a strong baseline predictor of scar formation. The blocked fluorescence could have been the result of deep sub-RPE hemorrhage or deep fibrosis not visible on color photographs.

In a previous CATT report, we described a strong association between decreased visual acuity at the end of 1 year and the presence of intraretinal fluid but not subretinal or

sub-RPE fluid on OCT.[1] Thus, it is surprising that subretinal fluid is independently associated with scar formation by the end of 2 years because scar was also associated with decreased visual acuity at 2 years. It is possible that with a longer period of observation, subretinal fluid also could affect visual acuity through scar formation.

In our study, we did not see a significant association of RAP with scar after adjusting for other factors, although the univariate analysis (Table 1, available at www.aaojournal.org) showed that eyes with RAP at baseline developed fewer scars when compared with eyes that did not have RAP. This observation could be related to the relatively smaller RAP lesions or their common association with occult CNV, which forms fewer scars than classic CNV. A relatively small study that followed the natural history of RAP lesions for a mean duration of 20 months found subretinal fibrosis on FA and red-free photographs in 10 of 16 eyes (62%),[38] but a more recent study reported that only one third of the RAP lesions treated with three 0.5-mg intravitreal injections of ranibizumab and followed up for 3 years developed retinal scarring.[39] Although further investigation is warranted, these data suggest that anti-VEGF treatment prevents scar formation from RAP lesions.

We did not find an association between scar and genotypes for 5 SNPs (complement factor H, age-related maculopathy susceptibility 2, high temperature requirement factor A1, complement component 3, and toll-like receptor 3) that are known to have strong associations with the development of AMD. Further studies to investigate the expression of connective tissue growth factor and other fibrosis-associated cytokines, such as transforming growth factor ß, in eyes with nvAMD and exploration of association with known genomic predictors of excessive scar formation, such as keloids, may reveal genetic variants that may mitigate development of scar in nvAMD.[40]

In conclusion, a thorough understanding of the presenting morphology, history, and subsequent morbidity of nvAMD targeted by intravitreal anti-VEGF injections is essential to predict outcomes. Angiographic characteristics, such as the classic CNV phenotype, blocked fluorescence, and larger CNV lesions at baseline, and OCT characteristics, such as greater retinal thickness and subretinal tissue complex thickness, foveal subretinal fluid, and SHRM, predict increased risk of scar formation. Because scar formation is strongly associated with poor visual outcomes, investigation of potential treatments that reduce the formation of macular scar in AMD could prevent the loss of visual function.

References

1. Jaffe GJ, Martin DF, Toth CA, et al; Comparison of Age-related Macular Degeneration Treatments Trials Research Group. Macular morphology and visual acuity in the Comparison of Age-related Macular Degeneration Treatments Trials. Ophthalmology 2013;120:1860–70.
2. Bressler NM, Frost LA, Bressler SB, et al. Natural course of poorly defined choroidal neovascularization associated with macular degeneration. Arch Ophthalmol 1988;106:1537–42.
3. Wong TY, Chakravarthy U, Klein R, et al. The natural history and prognosis of neovascular age-related macular degeneration: a systematic review of the literature and meta-analysis. Ophthalmology 2008;115:116–26.
4. Pauleikhoff D. Neovascular age-related macular degeneration: natural history and treatment outcomes. Retina 2005;25:1065–84.
5. Sivaprasad S, Saleh GM, Jackson H. Does lesion size determine the success rate of photodynamic therapy for age-related macular degeneration? Eye (Lond) 2006;20:43–5.
6. AMDRT Research Group. The Age-Related Macular Degeneration Radiotherapy Trial (AMDRT): one year results from a pilot study. Am J Ophthalmol 2004;138:818–28.
7. Trikha R, Morse LS, Zawadzki RJ, et al. Ten-year follow-up of eyes treated with stereotactic fractionated external beam radiation for neovascular age-related macular degeneration. Retina 2011;31:1303–15.
8. Curtis LH, Hammill BG, Qualls LG, et al. Treatment patterns for neovascular age-related macular degeneration: analysis of 284 380 Medicare beneficiaries. Am J Ophthalmol 2012;153:1116–24.
9. Cohen SY, Oubraham H, Uzzan J, et al. Causes of unsuccessful ranibizumab treatment in exudative age-related macular degeneration in clinical settings. Retina 2012;32:1480–5.
10. CATT Research Group. Ranibizumab and bevacizumab for neovascular age-related macular degeneration. N Engl J Med 2011;364:1897–908.
11. Grunwald JE, Daniel E, Ying GS, et al; CATT Research Group. Photographic assessment of baseline fundus morphologic features in the Comparison of Age-Related Macular Degeneration Treatments Trials. Ophthalmology 2012;119:1634–41.
12. DeCroos FC, Toth CA, Stinnett SS, et al; CATT Research Group. Optical coherence tomography grading reproducibility during the Comparison of Age-related Macular Degeneration Treatments Trials. Ophthalmology 2012;119:2549–57.
13. Kaiser PK, Blodi BA, Shapiro H, Acharya NR; MARINA Study Group. Angiographic and optical coherence tomographic results of the MARINA study of ranibizumab in neovascular age-related macular degeneration. Ophthalmology 2007;114:1868–75.
14. Benjamini Y, Hochberg Y. Controlling the false discovery rate: a practical and powerful approach to multiple testing. J R Stat Soc Series B (Methodol) 1995;57:289–300.
15. Beaumont PE, Kang HK. Lesion morphology in age-related macular degeneration and its therapeutic significance. Arch Ophthalmol 2006;124:807–12.
16. Rosenfeld PJ, Shapiro H, Tuomi L, et al; MARINA and ANCHOR Study Groups. Characteristics of patients losing vision after 2 years of monthly dosing in the phase III ranibizumab clinical trials. Ophthalmology 2011;118:523–30.
17. Bressler NM, Bressler SB, Fine SL. Age-related macular degeneration. Surv Ophthalmol 1988;32:375–413.
18. Zauberman H, Ivry M, Sachs U. The macular vessels in pre-disciform and disciform senile macular degeneration. Am J Ophthalmol 1970;70:498–504.
19. Gregor Z, Bird AC, Chisholm IH. Senile disciform macular degeneration in the second eye. Br J Ophthalmol 1977;61:141–7.
20. Green WR, Enger C. Age-related macular degeneration histopathologic studies. The 1992 Lorenz E. Zimmerman Lecture. Ophthalmology 1993;100:1519–35.
21. Kim SY, Sadda S, Pearlman J, et al. Morphometric analysis of the macula in eyes with disciform age-related macular degeneration. Retina 2002;22:471–7.

22. Hogg R, Curry E, Muldrew A, et al. Identification of lesion components that influence visual function in age related macular degeneration. Br J Ophthalmol 2003;87:609–14.

23. Brown DM, Kaiser PK, Michels M, et al; ANCHOR Study Group. Ranibizumab versus verteporfin for neovascular age-related macular degeneration. N Engl J Med 2006;355: 1432–44.

24. Rosenfeld PJ, Brown DM, Heier JS, et al; MARINA Study Group. Ranibizumab for neovascular age-related macular degeneration. N Engl J Med 2006;355:1419–31.

25. Heier JS, Boyer D, Nguyen QD, et al; CLEAR-IT 2 Investigators. The 1-year results of CLEAR-IT 2, a phase 2 study of vascular endothelial growth factor Trap-Eye dosed as-needed after 12-week fixed dosing. Ophthalmology 2011;118:1098–106.

26. Kaiser PK, Brown DM, Zhang K, et al. Ranibizumab for predominantly classic neovascular age-related macular degeneration: subgroup analysis of first-year ANCHOR results. Am J Ophthalmol 2007;144:850–7.

27. Unver YB, Yavuz GA, Bekiroğlu N, et al. Relationships between clinical measures of visual function and anatomic changes associated with bevacizumab treatment for choroidal neovascularization in age-related macular degeneration. Eye (Lond) 2009;23:453–60.

28. Wilgus TA, Ferreira AM, Oberyszyn TM, et al. Regulation of scar formation by vascular endothelial growth factor. Lab Invest 2000;8:579–90.

29. O'Neill EC, Qin Q, Van Bergen NJ, et al. Antifibrotic activity of bevacizumab on human Tenon's fibroblasts in vitro. Invest Ophthalmol Vis Sci 2010;51:6524–32.

30. Li Z, Van Bergen T, Van de Veire S, et al. Inhibition of vascular endothelial growth factor reduces scar formation after glaucoma filtration surgery. Invest Ophthalmol Vis Sci 2009;50:5217–25.

31. Memarzadeh F, Varma R, Lin LT, et al. Postoperative use of bevacizumab as an antifibrotic agent in glaucoma filtration surgery in the rabbit. Invest Ophthalmol Vis Sci 2009;50: 3233–7.

32. Van Geest RJ, Lesnik-Oberstein SY, Tan HS, et al. A shift in the balance of vascular endothelial growth factor and connective tissue growth factor by bevacizumab causes the angiofibrotic switch in proliferative diabetic retinopathy. Br J Ophthalmol 2012;96:587–90.

33. Kuiper EJ, de Smet MD, van Meurs JC, et al. Association of connective tissue growth factor with fibrosis in vitreoretinal disorders in the human eye. Arch Ophthalmol 2006;124:1457–62.

34. Stevens TS, Bressler NM, Maguire MG, et al. Occult choroidal neovascularization in age-related macular degeneration. A natural history study. Arch Ophthalmol 1997;115:345–50.

35. Scupola A, Coscas G, Soubrane G, Balestrazzi E. Natural history of macular subretinal hemorrhage in age−related macular degeneration. Ophthalmologica 1999;213:97–102.

36. Avery RL, Fekrat S, Hawkins BS, Bressler NM. Natural history of subfoveal subretinal hemorrhage in age-related macular degeneration. Retina 1996;16:183–9.

37. Hwang JC, Del Priore LV, Freund KB, et al. Development of subretinal fibrosis after anti-VEGF treatment in neovascular age-related macular degeneration. Ophthalmic Surg Lasers Imaging 2011;42:6–11.

38. Viola F, Massacesi A, Orzalesi N, et al. Retinal angiomatous proliferation: natural history and progression of visual loss. Retina 2009;29:732–9.

39. Rouvas AA, Chatziralli IP, Theodossiadis PG, et al. Long-term results of intravitreal ranibizumab, intravitreal ranibizumab with photodynamic therapy, and intravitreal triamcinolone with photodynamic therapy for the treatment of retinal angiomatous proliferation. Retina 2012;32:1181–9.

40. Nakashima M, Chung S, Takahashi A, et al. A genome-wide association study identifies four susceptibility loci for keloid in the Japanese population. Nat Genet 2010;42:768–71.

Footnotes and Financial Disclosures

[1] Department of Ophthalmology, University of Pennsylvania, Philadelphia, Pennsylvania.

[2] Department of Ophthalmology, Duke University, Durham, North Carolina.

[3] Cole Eye Institute, Cleveland Clinic, Cleveland, Ohio.

[4] Department of Ophthalmology, University of Colorado-Denver, Aurora, Colorado.

Correspondence:

Ebenezer Daniel, MBBS, PhD, Fundus Photograph Reading Center, Department of Ophthalmology, University of Pennsylvania, 3535 Market Street, Suite 700, Philadelphia, PA 19104 E-mail: ebdaniel@mail.med.upenn.edu.